DOI: 10.4149/km_2010_4_233

An improved, stress-dependent, energy-barrier model for the creep of 9Cr-1Mo-0.2V steel under disc-bend loading

A. Nagode[1]*, L. Kosec[1], M. Jenko[2], B. Ule[2]†

[1] *Faculty of Natural Sciences and Engineering, Aškerčeva cesta 12, SI-1000 Ljubljana, Slovenia*
[2] *Institute of Metals and Technology, Lepi pot 11, SI-1000 Ljubljana, Slovenia*

Received 24 September 2008, received in revised form 21 July 2009, accepted 4 May 2010

Abstract

In this paper we describe the creep behaviour of 9Cr-1Mo-0.2V steel under disc-bend loading, also known as the small-punch method. An improved power-law, stress-dependent, energy-barrier model was used to describe the creep behaviour of 9Cr-1Mo-0.2V steel because the characteristics of this steel cannot be accurately described using a simple, Arrhenius-type power law. A good correlation between the calculated values from the improved model and the experimental data was obtained for discs of different thickness, i.e., 0.50 mm, 0.47 mm and 0.44 mm. We found that the optimum disc thickness for our small-punch device was 0.50 mm. The stress-dependent, apparent activation energy of creep for a disc thickness of 0.50 mm decreased from $\sim 543\,\mathrm{kJ\,mol^{-1}}$ to $\sim 535\,\mathrm{kJ\,mol^{-1}}$ as the load increased from 350 N to 550 N, with the load exponent equal to 4.5. These values are very close to the results from conventional, uniaxial creep tests.

K e y w o r d s: small-punch, 9Cr-1Mo-0.2V steel, creep equation, stress-dependent activation energy, Monkman-Grant relationship

1. Introduction

Since there is an increasing demand for power plants with higher efficiency it is important to find the most economical material solutions for steam plants operating at high temperatures and high pressures. As a result, creep-resistant steel has been the subject of extensive investigations. The 9Cr-1Mo-0.2V steel is widely used for high-temperature pipe work components in advanced power plants because it offers a combination of a good high-temperature creep strength, a high resistance to corrosion cracking, a low oxidation rate and good weldability [1–3]. It is already known that the creep behaviour of 9Cr-1Mo-0.2V steel cannot be described properly with a simple Arrhenius-type power law since the activation energy Q_c, defined as $\left[\frac{\partial \ln \dot{\varepsilon}_{\min}}{\partial\,(-1/RT)}\right]_\sigma$, shows a strong stress dependence, while the stress exponent n, defined as $\left(\frac{\partial \ln \dot{\varepsilon}_{\min}}{\partial \ln \sigma}\right)_T$, has a strong temperature dependence [4–6]. The high values obtained for the activation energies, which in the case of 9Cr-1Mo-0.2V steel exceed $800\,\mathrm{kJ\,mol^{-1}}$, have no physical meaning because they cannot be attributed to any known creep mechanism in this kind of steel. Čadek and co-workers [4, 5] made an attempt to interpret such behaviour by applying the Rösler-Arzt concept [7] for the thermally activated detachment of dislocations from carbide particles as a rate-controlling process. However, the modelling of creep behaviour using this concept was demonstrated to be ineffective. Later, Spigarelli [6] tried to explain the creep behaviour of 9Cr-1Mo-0.2V steel by incorporating a threshold stress concept, which satisfactorily describes the creep behaviour; however, the threshold stress is not a good material parameter since it often varies with the temperature and/or the applied stress, and in some cases it can even change its sign.

The influence of multi-axially stressed state on the lifetime of cylindrical notched specimen of the same kind of steel under creep loading was studied by Knésl et al. [8]. Using Norton power-law model for describ-

*Corresponding author: tel.: 0038612000433; fax: 0038614704560; e-mail address: ales.nagode@omm.ntf.uni-lj.si

ing steady state stage he found that the lifetime of notched specimen was controlled by two parameters. The first one corresponds to applied load level and determines the lifetime of specimen with the same geometry but without the notch, while the second parameter expresses the influence of size and geometry of the notch.

Recently, Ule and Nagode [9–11] have introduced an improved power-law, stress-dependent, energy-barrier model for describing the creep behaviour of 9Cr-1Mo-0.2V steel. The improvement over the standard model [12] is based, first, on the hypothesis that the application of stress also affects the energy barrier to be overcome when a local region transits from the initial state to the final state, and second, by applying a simple power function of stress instead of a hyperbolic sine function in the model-based equation. However, there is an additional advantage from taking into consideration the variation of the activation volume with temperature. The linear proportionality between the activation volume and T was confirmed, which simplified the equation into the following form:

$$\dot{\varepsilon}_{\min} = C_1 \left(\frac{\sigma}{G}\right)^n \exp\left(-\frac{Q_{\mathrm{c\,max}} - C_2\,(\sigma/G)}{RT}\right), \quad (1)$$

where $\dot{\varepsilon}_{\min}$ is the minimum creep rate, σ is the applied stress, $Q_{\mathrm{c\,max}}$ is the apparent activation energy, i.e., the limiting value of the activation energy when $\sigma \rightarrow 0$, G is the shear modulus (G (MPa) = 97400 – 0.039T), n is the stress exponent, T is the absolute temperature, R is the universal gas constant (R = 8.314 J mol^{-1} K^{-1}), and C_1 (s^{-1}) and C_2 (J mol^{-1}) are constants. This model has been used quite successfully for a description of the creep behaviour of 9Cr-1Mo-0.2V steel during conventional, uniaxial, tensile creep tests under a constant load as well as under a constant stress [9–11]. The obtained activation energies are found to be less stress dependent; however, they are still high and, thus, in good agreement with the literature data [4–6], while the stress exponent, between 4.5 and 5.5, is somewhat smaller than the values from the literature [4–6].

For measuring the creep properties of single parts of welded joints or when removing a larger amount of material to make a specimen, it is common to cause irreparable damage to the mechanical part, and it is impossible to carry out a conventional creep test with a cylindrical specimen. Thus, a number of test techniques have been under development for the purpose of extracting the mechanical properties from small-volume specimens [13, 14]. One of these techniques is the miniaturized disc-bend test, also known as the small-punch test. In this test a thin, circular disc is supported over a recessed hole and forced under constant load to deform into the hole by means of a spherically shaped punch. This gives rise to a rotary symmetrical, multi-axially stressed state in the specimen. The initial, large and rapid hot deformation of the disc has no effect on the regularity or the duration of the creep process. However, the duration of the creep process is influenced by the thickness of the disc as well as by the ratio between the disc thickness and the die clearance. Therefore, the condition $\theta_0 \leq \mathrm{Cl}$ (where θ_0 is the disc thickness and Cl is the so-called die clearance) has to be fulfilled in order to measure the creep properties correctly [15]. A comparison between the static disc loading P during the small-punch creep test and the tensile stress σ during a conventional, uniaxial, tensile creep test confirmed the most likely linear dependence between σ/P and $1/\theta_0$ described by the following relation [16]:

$$\sigma = P/(2.33\delta_{\mathrm{r}} \cdot \theta_0), \quad (2)$$

where δ_{r} is the deflection detected at the moment of rupture.

The latest investigations on numerous metals carried out by Milička and Dobeš [17] show a good empirical relation between σ during a conventional, uniaxial, tensile creep test and P during a small-punch creep test that results in an identical time-to-rupture at a given temperature, i.e.,

$$P = k\sigma, \quad (3)$$

where the proportionality factor $k = 2.85$ for 9Cr-1Mo-0.2V steel was obtained if P was expressed in N and σ in MPa [17]. The proportionality factor k is probably independent on the temperature; however, it is dependent on the thickness of the disc θ_0 and the geometry of the actual small-punch device, which has recently been confirmed by Milička and Dobeš [18].

In this paper we tried to use an improved power-law, stress-dependent, energy-barrier model to describe the creep behaviour of 9Cr-1Mo-0.2V steel during small-punch creep testing. During this investigation we also attempted to determine the effect of the disc thickness as well as the relation between the minimal deflection rate $\dot{\delta}_{\min}$ and the time-to-rupture t_{r} using the Monkman-Grant relation [19].

2. Experimental

The 9Cr-1Mo-0.2V steel with the chemical composition 0.104 C, 0.30 Si, 0.43 Mn, 9.01 Cr, 0.01 Ni, 0.95 Mo, 0.22 V, 0.06 Nb and balance Fe (all values in wt.%) was used in our research. In order to homogenize the microstructure, the investigated steel was subjected to an additional two-stage heat treatment (1050 ℃ for 1 h, vacuum cooling + 750 ℃ for 1 h, vacuum cooling). The initial, tempered martensite ferritic microstructure of the investigated steel is shown

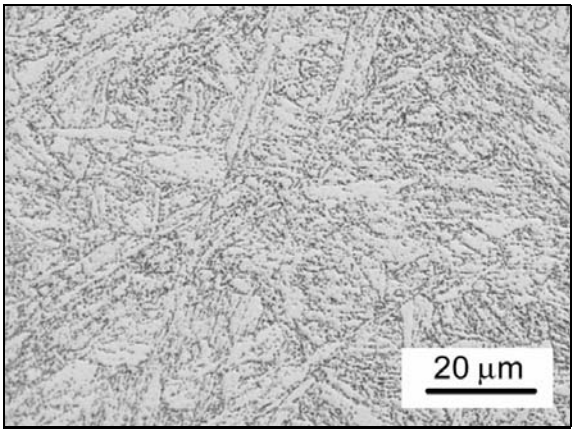

Fig. 1. Tempered martensite ferritic microstructure of the investigated 9Cr-1Mo-0.2V steel.

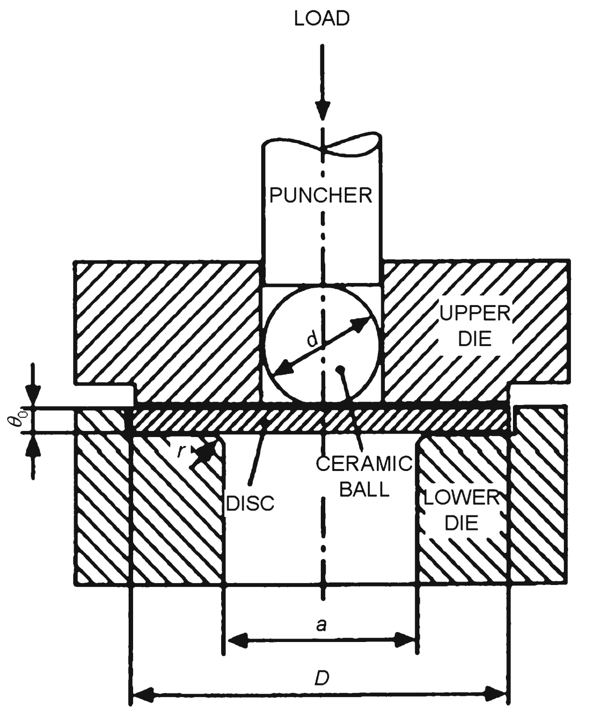

Fig. 2. Schematic illustration of the central part of the small-punch testing equipment.

in Fig. 1. The disc test specimens were prepared from a pipe with an outer radius of 325 mm and a wall thickness of 15 mm. The diameter of the disc test specimens was 8 mm and thickness was 0.50, 0.47 and 0.44 mm. These discs were cut from the wall of the pipe in such a way that the normal to the disc surface was parallel to the axis of the pipe. All the discs were ground and polished to 1200 grit.

The experimental work consisted of a test with the small-punch equipment. The central part of this equipment is shown in Fig. 2. The tests were performed at

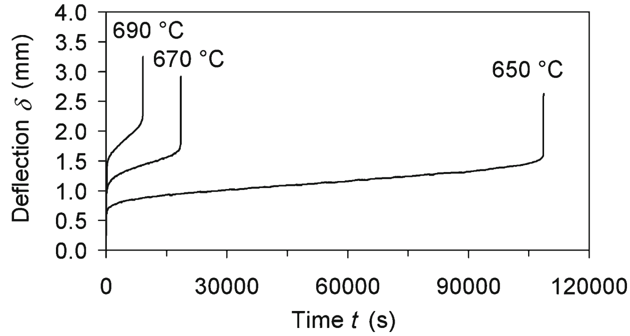

Fig. 3. Example of small-punch creep curves, i.e., the time dependence of the central deflection of a disc of thickness 0.50 mm under a load of 450 N and temperatures of 650 °C, 670 °C and 690 °C.

temperatures of 650, 675 and 690 °C and at loads from 350 N to 550 N. For each of the test conditions at least three measurements were made. The discs were placed on the central axis of the lower die of the specimen holder and fixed by the upper die to provide a loose fit, i.e., neglecting the friction between the upper die and the specimen. During the test, a constant load acted on the disc by means of a ceramic ball of diameter $d = 2.5$ mm, so that the specimen deflected into the cylindrical hole in the middle of the lower die. The diameter of the hole was $a = 4$ mm, and its shoulder radius was $r = 0.2$ mm. The temperature of the specimen was measured with a thermocouple, placed as close as possible to the specimen, the permissible variation in the temperature being ±1 °C. The displacement of the punch, i.e. the central deflection of the disc specimens, was measured using an inductive transducer with a high measuring accuracy (±1 μm). This displacement was recorded continuously on a computer.

3. Results and discussion

The creep curves corresponding to the small-punch test specimens, shown in Fig. 3, differ from the well-known shape of conventional creep curves mainly in the initial, very steep part of the small-punch creep curves. However, the minimum deflection rate can be evaluated from the curves representing the time dependence of the deflection rate (Fig. 4), which are obtained by differentiating the creep curves ($\mathrm{d}\delta/\mathrm{d}t$).

The relationship between the minimum deflection rate $\dot{\delta}_{\min}$ and the time-to-rupture t_r was plotted for the small-punch disc specimens of different thicknesses, θ_0, i.e., 0.50, 0.47 and 0.44 mm, in the bi-logarithmic diagram shown in Fig. 5. In this way, the perfect validity of the modified Monkman-Grant relation [19] in which the minimum deflection rate $\dot{\delta}_{\min}$ is used instead of the minimum creep rate $\dot{\varepsilon}_{\min}$ was experimentally confirmed. The modified relation thus obtained is

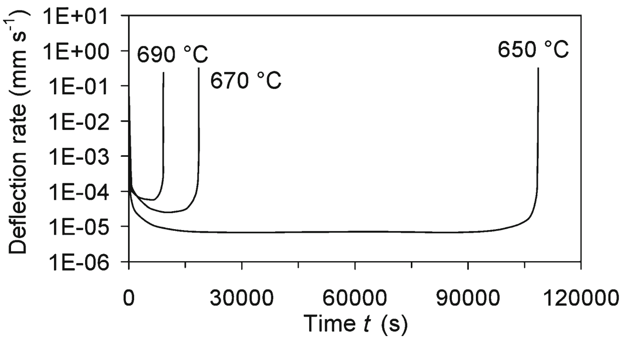

Fig. 4. Time dependence of the deflection rate of a disc $\dot{\delta}$ of thickness 0.50 mm at a load of 450 N and temperatures of 650 ℃, 670 ℃ and 690 ℃.

$$t_{\mathrm{r}} = M\dot{\delta}_{\mathrm{min}}^{-p}. \quad (4)$$

A very high correlation coefficient was obtained ($R^2 \sim 0.96$ to ~ 0.99) for all the disc thicknesses.

Since for all three disc thicknesses the Monkman-Grant parameter p is close to 1, the minimum deflection rate $\dot{\delta}_{\mathrm{min}}$ is almost inversely proportional to the time-to-rupture t_{r}. Thus, a minimum deflection rate $\dot{\delta}_{\mathrm{min}}$, i.e., a minimum creep rate $\dot{\varepsilon}_{\mathrm{min}}$ in an improved power-law, stress-dependent, energy-barrier model (Eq. (1)) can be replaced with the time-to-rupture t_{r}, so that Eq. (1) transforms to:

$$t_{\mathrm{r,SP}} = C_1 \left(\frac{\sigma}{G}\right)^{-n_{\mathrm{SP}}} \exp\left(\frac{Q_{\mathrm{c\,max}} - C_2\,(\sigma/G)}{RT}\right). \quad (5)$$

The exact meaning of this stress in Eq. (5) is not yet known, but it could represent a scalar value of those stress components that are crucial for the time-to-rupture of the disc and thus it is called the critical stress. Although the distribution of the stress in the disc is rotary symmetrical, the multi-axial stress state, as well as the deformation state, is heterogeneous. Therefore, the most convenient stress in Eq. (5) seems to be the maximum effective stress $\bar{\sigma}_{\mathrm{max}}$ for which the von Mises effective stress was adopted as well as the assumption that not the spherical part, but only the deviatoric part of the stress tensor has an influence on the creep behaviour. The value of this stress is not known, since only the load P is measured for a particular disc thickness and geometry of the small-punch testing device. Since Milička and Dobeš [17, 18] experimentally determined the linear dependence between the stress σ during a conventional, uniaxial, tensile creep test and the load P during a small-punch creep test, which results in an identical time-to rupture t_{r} (Eq. (3)), Eq. (5) can be rearranged to:

$$t_{\mathrm{r,SP}} = C_1 \left(\frac{P}{C_3}\right)^{-n_{\mathrm{SP}}} \exp\left(\frac{Q_{\mathrm{c\,max}} - P/C_2}{RT}\right), \quad (6)$$

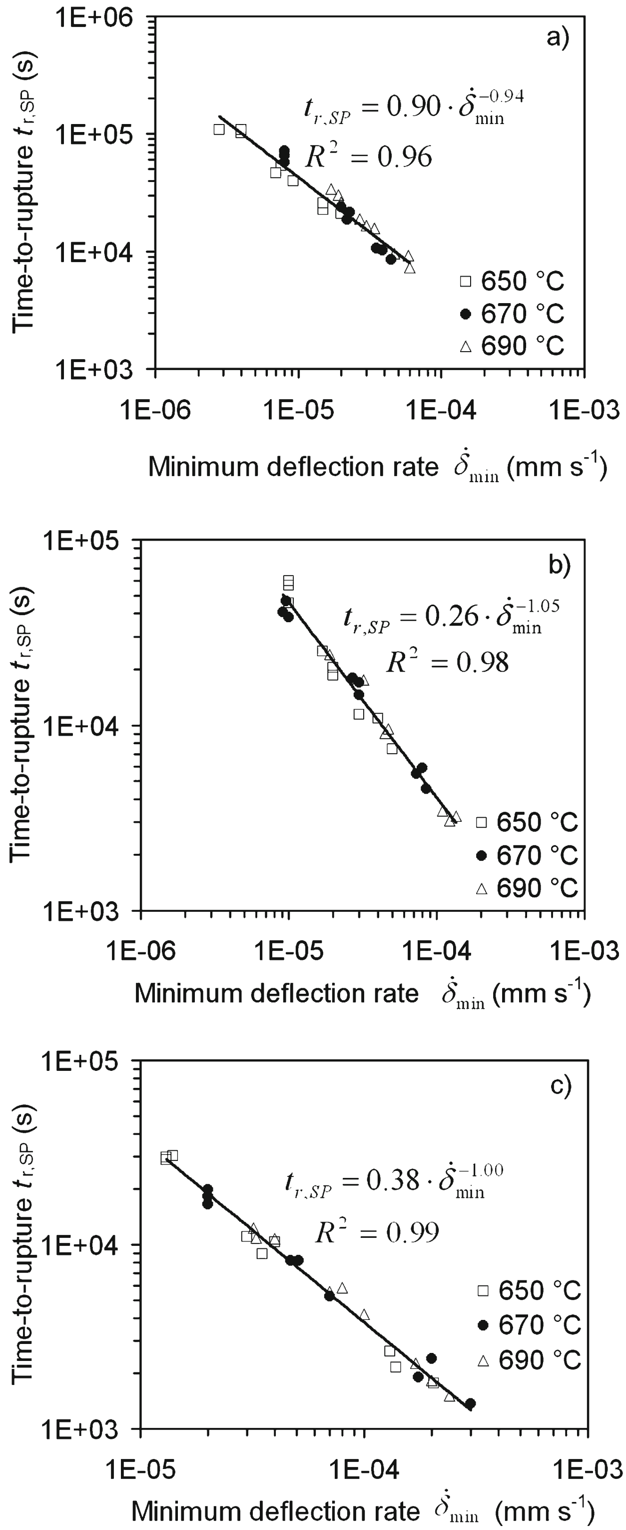

Fig. 5. Dependence of the time-to-rupture t_{r} on the minimum deflection rate $\dot{\delta}_{\mathrm{min}}$ for different disc thicknesses: a) $\theta_0 = 0.50$ mm, b) $\theta_0 = 0.47$ mm and c) $\theta_0 = 0.44$ mm.

where P is the applied load when measuring the creep properties of the disc, C_1, C_2 and C_3 are the thickness-

Table 1. Values of the constants C_1, C_2 and C_3, the apparent activation energies $Q_{c\,max}$ and the load exponents n_{SP} for the different disc thicknesses

θ_0 (mm)	C_1 (s)	C_2 (mol m^{-1})	C_3 (N)	$Q_{c\,max}$ (J mol^{-1})	n_{SP}
0.50	2.95×10^{-16}	2.04×10^{-2}	2.87	560 000	4.5
0.47	5.85×10^{-16}	1.52×10^{-2}	2.67	560 000	4.5
0.44	1.61×10^{-15}	1.11×10^{-2}	2.45	560 000	4.5

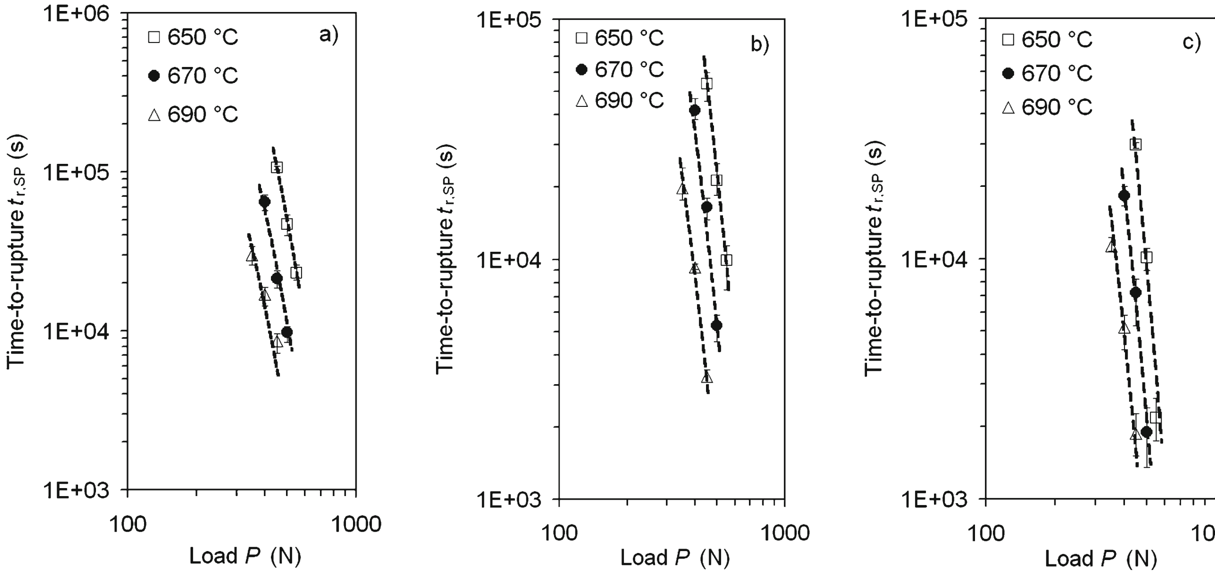

Fig. 6. Correlation of the model with the experimental data for different disc thicknesses: a) $\theta_0 = 0.50$ mm, b) $\theta_0 = 0.47$ mm and c) $\theta_0 = 0.44$ mm. The points represent the experimental values, whereas the dashed lines represent the values obtained from Eq. (6).

-dependent constants, $Q_{c\,max}$ is the apparent activation energy, i.e., the limiting value of the activation energy when $P \to 0$, and n_{SP} is the load exponent.

The values of the constants C_1, C_2 and C_3, as well as the apparent activation energies $Q_{c\,max}$ and the load exponents n_{SP} were obtained by means of a statistical multi-regression analysis of the creep-test data and are listed in Table 1. However, these constants have to be considered as fitting parameters in the applied equation, which is still semi-empirical but theoretically well founded and that satisfactorily describes the creep behaviour of 9Cr-1Mo-0.2V steel under disc-bend loading.

In Fig. 6, the times-to-rupture t_r calculated from the improved power-law, stress-dependent, energy-barrier model (Eq. (4)) are plotted against the applied load P on a bi-logarithmic scale together with our experimental data for the different disc thicknesses, i.e., 0.50 mm, 0.47 mm and 0.44 mm. It is clear that there is a good correlation between the model and the experimental data.

As can be seen from Table 1, the apparent activation energies $Q_{c\,max}$ and the load exponents n_{SP} are equal for all three disc thicknesses, while the constants C_1, C_2 and C_3 are dependent on the disc thicknesses.

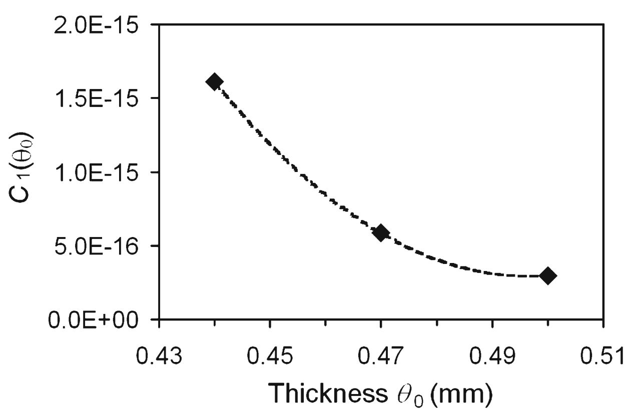

Fig. 7. Dependence of the constant C_1 on the disc thickness θ_0.

The dependence of the constant C_1 on the disc thickness (Fig. 7) can be expressed with the following polynomial equation, obtained from a computer-assisted analysis:

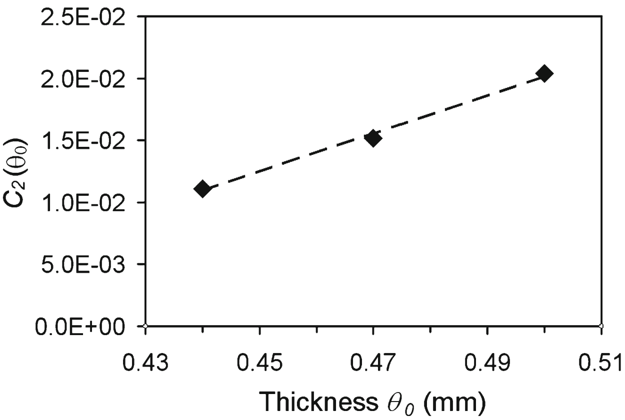

Fig. 8. Linear dependence of the constant C_2 on the disc thickness θ_0.

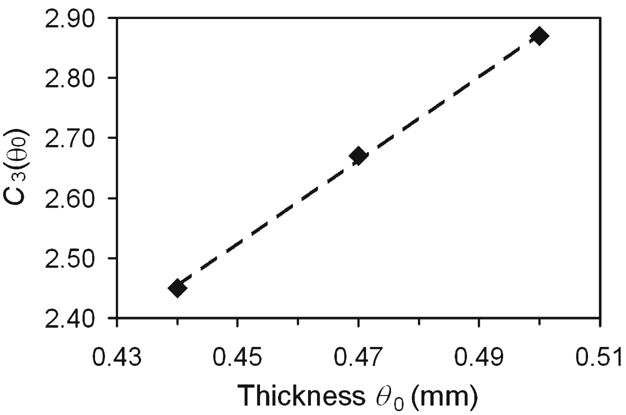

Fig. 9. Linear dependence of the constant C_3 on the disc thickness θ_0.

$$C_1(\theta_0) = 4.0833 \times 10^{-13}\theta_0^2 - 4.0575 \times 10^{-13}\theta_0 + 1.0109 \times 10^{-13}. \quad (7)$$

The constant C_1 includes the influence of the geometry of the small-punch device (the disc thickness, the diameter of the hole in the lower die, the diameter of the ceramic ball, the die clearance or the ratio between them). From Fig. 7 it is clear that at some disc thickness (between ~ 0.48 mm and ~ 0.50 mm) the constant C_1 becomes almost independent on the disc thickness. Since the maximum disc thickness is limited by the condition $\theta_0 \leq$ Cl [15], and thus it cannot exceed 0.50 mm, the optimum disc thickness for the actual small-punch device is, therefore, strictly determined.

The constant C_2 shows a linear dependence on the disc thickness (Fig. 8), and it can be described by the following equation:

$$C_2\,(\theta_0) = 0.16\theta_0 - 0.06. \quad (8)$$

The constant C_3 also shows a linear dependence on disc thickness (Fig. 9). For its description the following equation can be used:

$$C_3\,(\theta_0) = 7.000\theta_0 - 0.627. \quad (9)$$

By applying the above dependences of the constants C_1, C_2 and C_3 on the disc thickness, Eq. (6) can be rewritten in the form:

$$t_\mathrm{r} = \left(4.083\theta_0^2 - 4.058\theta_0 + 1.011\right) \times 10^{-13} \times \left(\frac{P}{7.000\theta_0 - 0.627}\right)^{-n_\mathrm{SP}} \times \exp\left(\frac{Q_{\mathrm{c\,max}} - P/(0.155\theta_0 - 0.057)}{RT}\right) \quad (10)$$

with the load exponent $n_\mathrm{SP} = 4.5$ and the apparent activation energy, i.e., the limiting value of the activation energy when $P \to 0$, $Q_{\mathrm{c\,max}} = 5.6 \times 10^5\ \mathrm{J\,mol^{-1}}$. The load P is expressed in N and the disc thickness θ_0 in mm.

The influence of the stress σ in Eq. (10) is expressed by the ratio P/θ_0. This is in accordance with Dobeš and co-workers [16], who already confirmed the linear dependence between σ/P and $1/\theta_0$, where σ is the stress during a conventional, uniaxial, tensile creep test, while P is the acting load on the disc of thickness θ_0 during a small-punch creep test that results in an identical time-to-rupture t_r at a given temperature.

If the optimum disc thickness for the actual small-punch device is chosen to be 0.50 mm, the equation for the time-to-rupture t_r can be written in more simplified form:

$$t_\mathrm{r} = D_1 \left(\frac{P}{\theta_0}\right)^{-n_\mathrm{SP}} \exp\left(\frac{Q_{\mathrm{c\,max}} - D_2(P\theta_0)}{RT}\right), \quad (11)$$

where D_1 ($D_1 = C_1 \left(\frac{C_3}{\theta_0}\right)^{n_\mathrm{SP}}$) and D_2 ($D_2 = \frac{\theta_0}{C_2}$) are constants calculated from Eq. (6). Hence, for disc thickness $\theta_0 = 0.50$ mm constants D_1 and D_2 are 7.67×10^{-13} s $(\mathrm{N\,mm^{-1}})^{4.5}$ and 24.51 $\mathrm{m^2\,mol^{-1}}$, respectively, the load exponent $n_\mathrm{SP} = 4.5$ and the limiting value of the apparent activation energy $Q_{\mathrm{c\,max}} = 560\ \mathrm{kJ\,mol^{-1}}$.

The value of the stress-dependent apparent activation energy of the creep Q_c for a disc thickness of 0.50 mm calculated from the expression ($Q_{\mathrm{c\,max}} - D_2(P/\theta_0)$) in Eq. (11) is 543 $\mathrm{kJ\,mol^{-1}}$ at an applied load $P = 350$ N, and 535 $\mathrm{kJ\,mol^{-1}}$ at an applied load $P = 500$ N. These activation energies for the creep are apparent activation energies, since they represent the stress-dependent activation energy of the slowest, dominant, rate-controlling mechanism of the proposed multiple-creep mechanisms.

Equation (11) shows that the critical stress, which is crucial for the time-to-rupture, can be approximated by a simple quotient P/θ_0. This is in agreement with the fact that the heterogeneous distribution of the critical stress and the strain in the disc is limited only in the circular area of disc, which is becoming thinner during the deflection of the disc, while the length of the circular area remains practically unchanged. The heterogeneous distribution of the strain, limited only in a well-defined circular area, was first confirmed by a numerical simulation of the disc during creep carried out by Rodič [20] and later experimentally documented by Komazai [21].

4. Conclusions

The results of the creep measurements on 9Cr-1Mo-0.2V steel using a small-punch creep test on discs of different thicknesses, i.e., 0.50 mm, 0.47 mm and 0.44 mm, are described.

– The relationship between the minimum deflection rate $\dot{\delta}_{\min}$ and the time-to-rupture t_r was studied. The perfect validity of the Monkman-Grant relationship was experimentally confirmed. The values of the Monkman-Grant parameter p are close to 1 (from ~ 0.93 to ~ 1.05) for all three disc thicknesses. Hence, the minimum deflection rate $\dot{\delta}_{\min}$, which is used instead of the minimum creep rate $\dot{\varepsilon}_{\min}$, is inversely proportional to the time-to-rupture t_r.

– For a description of the creep behaviour of 9Cr-1Mo-0.2V during a small-punch creep test an improved power-law, stress-dependent, energy-barrier model was used. This model, which has recently been satisfactorily used for conventional, uniaxial, creep tests, also shows a good correlation with the small-punch creep data, which gives rise to a rotary symmetric, multi-axially stressed state in the disc-bend specimen.

– It was found that the optimum disc thickness for an applied small-punch testing device was 0.50 mm. However, the disc thickness is not limited only by the maximum, with the condition $\theta_0 \leq$ Cl, but also by the minimum, which is ~ 0.48 mm for our small-punch device. Thus, for any small-punch device the disc thickness is strictly determined.

– The stress-dependent, apparent activation energies of creep Q_c for the optimum disc thickness of 0.50 mm decreases from $\sim 543\ \text{kJ mol}^{-1}$ to $\sim 535\ \text{kJ mol}^{-1}$ as the load P increases from 350 N to 550 N, while the load exponent n_{SP} is 4.5. These values of Q_c and n are very close to the results of the conventional creep tests that have been published recently. The stress-dependent, apparent activation energy is somewhat load-dependent, i.e., dependent on the quotient P/θ_0, which approximates the relevant stress in the disc that is crucial for the time-to-rupture of the disc.

References

[1] BLUM, W.—STRAUB, S.: Steel Research, *62*, 1991, p. 72.
[2] JONES, W. B.—HILLS, C. R.—POLONIS, D. H.: Metallurgical Transaction, *22A*, 1991, p. 1049.
[3] HALD, J.: Steel Research, *67*, 1996, p. 369.
[4] ČADEK, J.—ŠUSTEK, V.—PAHUTOVÁ, M.: Material Science and Engineering, *A225*, 1997, p. 22.
[5] ČADEK, J.—ŠUSTEK, V.: High Temperature Materials and Process, *16*, 1997, p. 97.
[6] SPIGARELLI, S.—CERRI, E.—BIANCHI, P.—EVANGELISTA, E.: Materials Science and Technology, *15*, 1999, p. 1433.
[7] RÖSLER, J.—ARZT, E.: Acta Metallurgica Materialia, *38*, 1990, p. 671.
[8] KNÉSL, Z.—PRECLIK, P.—RADON, J. C.: Kovove Mater., *41*, 2003, p. 84.
[9] ULE, B.—NAGODE, A.: Scripta Materialia, *57*, 2007, p. 405. doi:10.1016/j.scriptamat.2007.05.001
[10] NAGODE, A.—ULE, B.—JENKO, M.—KOSEC, L.: Steel Research Int., *78*, 2007, p. 638.
[11] ULE, B.—NAGODE, A.: Materials Science and Technology, 23, 2007, p. 1367. doi:10.1179/174328407X161187
[12] REED-HILL, R. E.—ABBASCHIAN, R.: Physical Metallurgy Principles. 3rd edition. Boston, PWS-KENT Publishing Company 1994.
[13] LUCAS, G. E.: Journal of Nuclear Materials, *117*, 1983, p. 327. doi:10.1016/0022-3115(83)90041-7
[14] LUCAS, G. E.: Metallurgical Transaction, *21A*, 1990, p. 1105.
[15] ULE, B.—ŠTURM, R.—LESKOVŠEK, V.: Materials Science and Technology, *19*, 2003, p. 1771. doi:10.1179/026708303225009463
[16] DOBEŠ, F.—MILIČKA, K.—ULE, B.—SUŠTAR, T.—BICEGO, V.—TETTAMANTI, S.—KOZLOWSKI, R. H.—KLAPUT, J.—WHELAN, M. P.—MAILE, K.—SCHWARZKOPF, C.: Engineering Mechanics, *5*, 1998, p. 157.
[17] MILIČKA, K.—DOBEŠ, F.: Materials Science Forum, *482*, 2005, p. 407.
[18] MILIČKA, K.—DOBEŠ, F.: International Journal of Pressure Vessels and Piping, *83*, 2006, p. 625.
[19] MONKMAN, F. C.—GRANT, N. J.: Proc. ASTM, *56*, 1956, p. 593.
[20] ULE, B.—ŠUŠTAR, T.—LOVRENČIČ SARAŽIN, M.—RODIČ, T.: In: Twelve Month Progress Report Period 1.2.1996 to 31.1.1997, COPERNICUS-Small Punch Test Method Assessment for the Determination of the Residual Creep Life of Service Exposed, "Small Punch", Project document classification code: 12MPR2_(IMT Ljubljana). Ljubljana, IMT 1997.
[21] KOMAZAI, S.—HASHIDA, T.—SHOJI, T.—SUZUKI, K.: Journal of Testing and Evaluation, *28*, 2000, p. 249.